

# A NEARLY MONO-ENERGETIC 6-7 MeV PHOTON CALIBRATION SOURCE

D. W. O. ROGERS

Physics Division, National Research Council of Canada, Montreal Road, Ottawa, Canada K1A 0R6

(Received 25 February 1982; accepted 26 May 1982)

**Abstract**—A photon source has been developed which delivers about 85% of its photon dose equivalent from photons with energies of 6.1, 6.9 and 7.1 MeV produced in the  $^{19}\text{F}(p, \alpha\gamma)^{16}\text{O}$  reaction. The source uses up to 50  $\mu\text{A}$  of 2.7 MeV protons incident on a 6  $\text{mg}/\text{cm}^2$  target of  $\text{CaF}_2$ . It produces a photon field with a dose equivalent rate of up to 6  $\text{mSv}/\text{h}$  (600  $\text{mrem}/\text{h}$ ) over a large area 100 cm from the target. The field can be calibrated in terms of photon fluence to within  $\pm 5\%$ . In common with other high-energy photon sources, there is considerable contamination of the field by knock-on electrons and scattered photons. Experiments with various filter materials and detailed Monte-Carlo calculations with the EGS electron-photon transport code have been done to investigate the importance of these contaminants.

## 1. INTRODUCTION

THIS PAPER reports on the development of a calibrated photon source which delivers most of its photon dose from  $\gamma$ -rays with energies between 6 and 7 MeV.

Neutrons with energies above 10 MeV react with oxygen in the water in the core of a nuclear reactor to create  $^{16}\text{N}$  via the  $^{16}\text{O}(n, p)^{16}\text{N}$  reaction. Since  $^{16}\text{N}$  has a 7.13-s half-life, a significant fraction of it is transported outside the main reactor shielding before decaying. The main decay modes are shown in Fig. 1. The  $\beta$  decays produce electrons with a maximum energy of 10.4 MeV. These are stopped in the pipe or pump walls and hence the major external radiation hazard comes from 6.13 MeV  $\gamma$ -rays which may contribute up to 50% of the dose at certain locations inside the containment at CANDU reactors. This observation shows the importance of developing accurate dosimetry techniques in this energy range.

As will be shown below, virtually none of the commercial instruments checked gave the expected readings. Many ion chambers over-responded by 50% and instruments based on

Geiger-Müller tubes over-responded typically by 150%. One reason for this is the knock-on electron contamination of the photon beam. This contamination is much more severe at 6 MeV than at  $^{60}\text{Co}$  energies or below.

The rest of Section 1 reviews previous

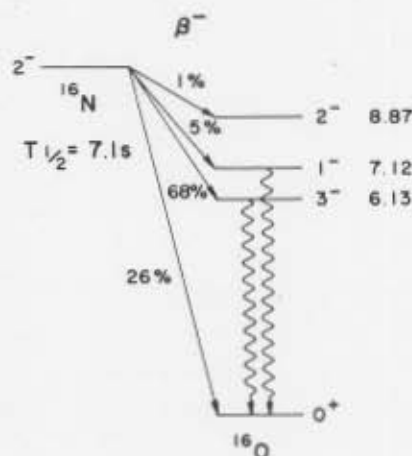


FIG. 1. Major decay modes of  $^{16}\text{N}$  taken from Aj77. Although the maximum  $\beta^-$  energy is 10.41 MeV they are generally stopped in pipe walls, leaving the 6.13 MeV  $\gamma$ -rays as the major source of concern in radiation protection.

work and describes the National Research Council of Canada source. In Section 2 there is a general discussion of the calibration technique which has been developed. This is followed by a description of the characteristics of the source in Section 3. Section 4 deals with the problem of contaminants in the calibration field.

### 1.2 Previous work

There have been two previous approaches used to create a 6 MeV calibration source. One involves passing water through a reactor core and circulating it through a disc shaped holder. Such sources at the University of Liverpool (Bi75) and University of Lowell (Ne80) have been calibrated in terms of exposure using ion chambers. The maximum exposure rates were of the order of  $5 \times 10^{-4} \text{ Ckg}^{-1} \text{ h}^{-1}$  [2R/h] and  $10^{-4} \text{ Ckg}^{-1} \text{ h}^{-1}$  [400 mR/h], respectively. The workers at Lowell covered the source with a  $1\frac{1}{2}$  in. steel plate to ensure the secondary-electron spectrum was similar to that found in the field.

A second approach has been adopted by Thompson *et al.* at the Berkeley Nuclear Laboratories (Th71). They produce 6 MeV photons from  $^{16}\text{O}$  by bombarding a thin target of  $^{19}\text{F}$  with a 340 keV beam of protons to induce the  $^{19}\text{F}(p, \alpha\gamma)^{16}\text{O}$  reaction. Calibration is achieved by counting the alpha particles and thereby deducing the photon fluence, or by using an ion chamber. They obtain fields of up to  $10^{-5} \text{ Ckg}^{-1} \text{ h}^{-1}$  [40 mR/h] 30 cm from the target.

### 1.3 The present approach

The source developed at the National Research Council of Canada (NRCC) also uses the  $^{19}\text{F}(p, \alpha\gamma)^{16}\text{O}$  reaction. The relevant reactions are shown in Fig. 2. Figure 3 shows a yield curve for this reaction taken with a thin target. Targets of  $\text{CaF}_2$  up to  $6 \text{ mg/cm}^2$  thick have been made by evaporating  $\text{CaF}_2$  from a tantalum boat heated to  $\sim 1300^\circ\text{C}$  and heating the target backing to  $150^\circ\text{C}$ . Using these thick targets essentially integrates the thin-target yield curve over the 700-keV region bounded above by the beam energy. Experimentally we find a maximum in the yield of 6-7 MeV photons from the thick tar-

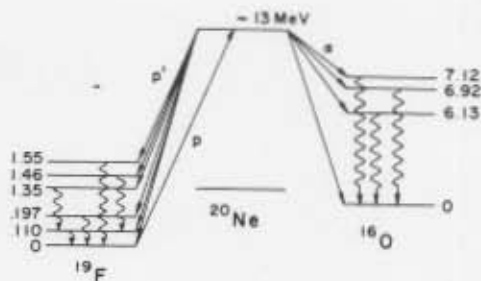


FIG. 2. The major decay channels involved in the  $^{19}\text{F}(p, \alpha\gamma)^{16}\text{O}$  source (taken from Aj77).

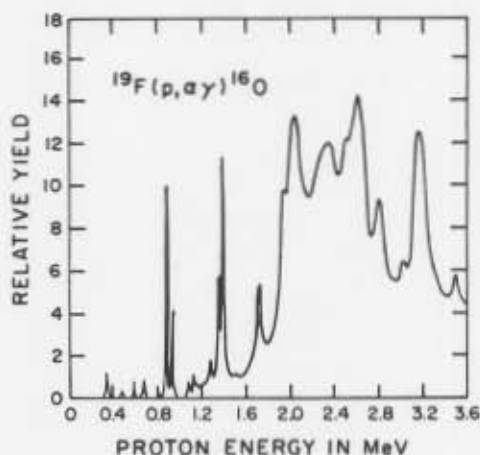


FIG. 3. The relative yield of 6-7 MeV  $\gamma$ -rays from a thin target of  $\text{CaF}_2$  bombarded by protons of varying energies (taken from Go60). The yield curve from the  $\approx 700$  keV thick targets used in the present source essentially integrates this curve and peaks at about 2.7 MeV.

get at about 2.7 MeV. Above this energy, 1.3-MeV contaminant photons from the  $^{19}\text{F}(p, p'\gamma)^{19}\text{F}$  reaction become significant. The optimum proton energy was therefore chosen as 2.7 MeV. In this configuration the yield of high-energy photons per  $\mu\text{A}$  of protons is several orders of magnitude higher than when 340-keV protons bombard a thin target, as is done by Thompson *et al.*

A 3.6-mm lead filter is wrapped around the target chamber to eliminate beam contamination by 110 and 197-keV  $\gamma$ -rays from the  $^{19}\text{F}(p, p'\gamma)^{19}\text{F}$  reaction. This filter attenuates the high energy photons by 16% and is a source of contamination electrons and photons (see Section 4).

## 2. THE CALIBRATION TECHNIQUE

The general question of what radiation quantity should be used for calibration purposes is a significant problem. Many radiation-protection instruments are calibrated in terms of exposure but at 6 MeV this quantity has virtually no meaning because of the extremely long range of the electrons set in motion (up to about 27 m in air). Although the medical-physics community has well developed procedures for using an exposure-calibrated ion chamber to measure absorbed dose, these procedures apply to small ion chambers making measurements in a phantom and thus do not apply to radiation-protection instruments.

Ideally, one would like a survey instrument located at a given point to provide the maximum dose equivalent in a human at that point—but what does “a human at that point” mean? This question is critical when considering a point source since the photon fluence decreases inversely with the square of the distance. ICRU Report 25 (ICRU76) would have the instrument read the dose equivalent index at that point, i.e. the maximum dose equivalent produced in a 30 cm-diameter tissue-equivalent sphere centered at that point. So, for example, for an instrument 100 cm from the NRCC source, the dose-equivalent index is defined for a spherical phantom centered at 100 cm and is given by the dose equivalent at a point roughly  $100 - 15 + 3 = 88$  cm from the source (the dose equivalent vs depth curve peaks at about 3 cm below the surface). While this may be the “correct” procedure, it has *not* been adopted here, both because it is not intuitive and because the same procedure is virtually never used to calibrate radiation protection instruments at  $^{60}\text{Co}$  or lower energies. Instead, the calibration procedure used here essentially measures the photon fluence at a point and converts to the maximum dose equivalent in a human phantom placed with its front surface at the same point (this will be referred to as the maximal dose equivalent).

In a photon field sufficiently intense to be useful for calibrating radiation-protection instruments, NaI and Ge(Li) detectors suffer

severe pile-up and deadtime problems. To avoid these problems a highly collimated NaI monitor detector is calibrated at low beam current ( $\sim 50$  nA) in terms of the photon fluence at the calibration point. For this a calibrated Ge(Li) and/or NaI detector is placed at the calibration point as shown in Fig. 4. Instrument calibrations are done by placing the instrument at the calibration point and running with up to  $50 \mu\text{A}$  of beam which still produces a negligible deadtime in the collimated monitor counter. This procedure has been checked by verifying that monitor counts scaled with the total beam charge over the range of beam currents involved.

The calibration has been based primarily on a  $5 \times 4$  in. NaI detector whose efficiency has been calculated using a detailed Monte-Carlo code (Ro82). The code has been verified to within an experimental uncertainty of 2% by using the associated-particle technique at the 340 keV resonance in the  $^{19}\text{F}(p, \alpha\gamma)^{16}\text{O}$  reaction to provide a known fluence of 6.13 MeV photons (Ma82). A secondary calibration has been based on a Ge(Li) detector for which an experimentally determined efficiency curve was available (Di81). The agreement between the two calibrations is well within the 10% uncertainty of the

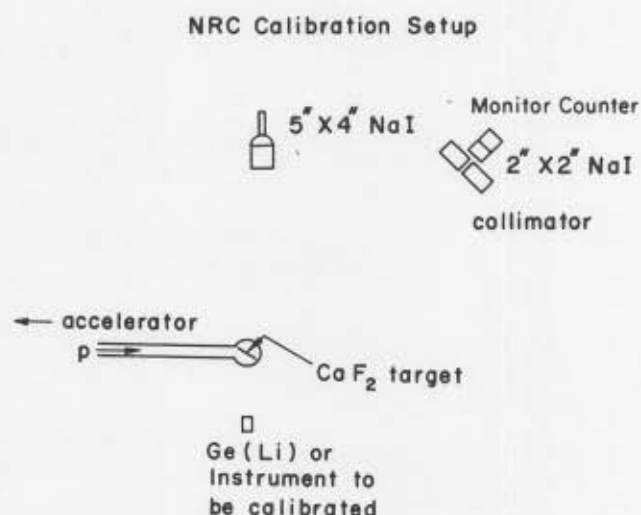


FIG. 4. The calibration setup employed at NRCC. Using 50 nA beams on target the collimated NaI is calibrated in terms of the fluence at the calibration point. The current is then increased to about  $30 \mu\text{A}$  for instrument calibration.

Ge(Li) calibration. Based on estimates of the present systematic uncertainties (count rate effects, statistics, deadtime effects, counter efficiencies), it is believed that the overall uncertainty in the fluence measurement is better than  $\pm 5\%$ .

The conversion from the measured fluence to maximal dose equivalent can be done using the factors given by Clairborne and Truby (C170) and the ANSI/ANS (AN77) or those given by the ICRP (ICRP71). Both of these publications have weaknesses and present conversion factors which differ by 6% at 7 MeV. The Clairborne-Truby results have been used. A correction factor is needed to account for the point-source nature of the field compared to the parallel beam assumed for the calculated conversion factors. Since the maximum on the depth dose curve occurs at  $\sim 3$  cm for 7-MeV photons incident on tissue, the correction factor reduces the maximal dose equivalent per incident photon by a factor  $[\text{SSD}/(\text{SSD} + 3)]^2$  where SSD is the source-to-surface distance (the factor is 0.89 at 50 cm, 0.94 at 100 cm).

After this work was complete, a set of fluence to maximal dose equivalent factors was computed using the EGS3 code (see Section 4.3.3). Near 7 MeV, the proper conversion factors are about 6% lower than those used in this work because of the consideration of electron transport (see Ro82c).

### 3. SOURCE CHARACTERISTICS

#### 3.1 Gamma-ray spectrum

Figure 5 shows a  $\gamma$ -ray spectrum taken with a Ge(Li) detector 1 m from the  $\text{CaF}_2$  target. The 6.92- and 7.12-MeV levels in  $^{16}\text{O}$  have such short lifetimes that they decay while the  $^{16}\text{O}$  is still moving after the  $\alpha$  decay of  $^{20}\text{Ne}$ . As a result their peak shapes are broadened by Doppler-shift effects. The width of the Doppler-broadened peaks ( $\sim 130$  keV) and their various shapes can be explained respectively by the reaction kinematics and angular distributions of the  $\alpha$  particles. The 6.13-eV peaks represent only 22% of the high-energy fluence despite the fact that they are the tallest (but sharpest) peaks. The 6.92 and 7.12-MeV peaks

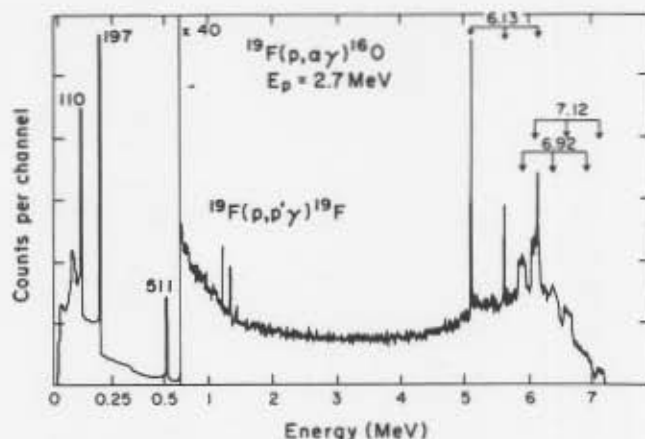


FIG. 5. The photon spectrum measured with a Ge(Li) detector 100 cm from the source with no filter present. The Doppler-broadened peaks at 6.9 and 7.1 MeV represent 78% of the high-energy intensity. The peaks near 1.3 MeV and at 197 and 110 keV are from the  $^{19}\text{F}(p, p'\gamma)^{19}\text{F}$  reaction. They contribute 3.8% as much dose as the 6-7 MeV  $\gamma$ -rays but this can be reduced to  $\sim 1.3\%$  using a lead filter. The 511 keV peak contributes 3.7% of the high-energy dose. Scattered photons and electrons are not evident due to their broad spectrum but are expected to contribute significantly to the total dose. Note the change in the energy scale.

represent 32 and 46% of the photon fluence respectively. A general discussion of the contaminant  $\gamma$ -rays is presented in Section 4.

#### 3.2 Source strength

The source strength depends on the quality and thickness of the  $\text{CaF}_2$  target and on the proton beam current it can sustain without deterioration. At  $90^\circ$  to the proton beam a "typical" good target produces  $1.8 \times 10^7$  photons above 6 MeV per steradian per  $\mu\text{C}$  of protons. On a good day the NRCC Van de Graaff can deliver a defocused 50- $\mu\text{A}$  beam of 2.7-MeV protons which the directly water-cooled  $\text{CaF}_2$  targets can withstand for many hours (but accidental beam focusing destroys the target in seconds). With a 50  $\mu\text{A}$  beam, the reaction generates a dose equivalent rate of 6 mSv/h (600 mrem/h) at 100 cm or 70 mSv/h (7 rem/h) at 30 cm.

#### 3.3 Field uniformity

From symmetry considerations the field must be uniform with respect to the azimu-

thal angle around the beam. However the beam defines a direction in space, making possible an angular distribution with respect to  $\theta$ , the photon polar angle relative to the beam direction.

Figure 6 shows the measured angular distribution. There is a 15% anisotropy between 0 and 90° but there is less than a 2% variation in the photon fluence within  $\pm 10^\circ$  of the calibration point at 90°. At 100 cm, this means the fluence across a flat 36 cm wide object centered at 90° would be virtually constant in view of the combination of distance and angular-distribution effects.

In summary, at 90° the photon fluence is uniform to better than 2% over a considerable area at 100 cm. However, the fact that it is a point source makes it somewhat difficult to deduce the dose equivalent at various points in an extended medium (short of a detailed Monte-Carlo calculation).

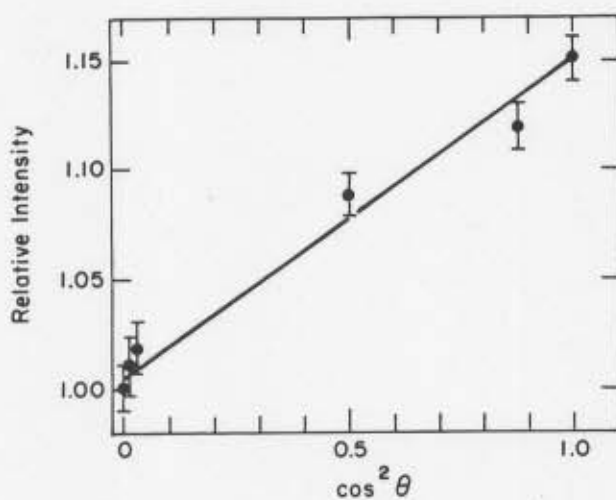


FIG. 6. Angular distribution of high-energy photons from the  $^{19}\text{F}(p,\alpha\gamma)^{16}\text{O}$  reaction for 2.7 MeV protons incident on a 6 mg/cm<sup>2</sup> CaF<sub>2</sub> target.  $\theta$  is the angle with respect to the beam axis. As is frequently the case, the angular distribution is linear in  $\cos^2 \theta$ . The photon intensity varies by only 5% between 90° and 57°.

#### 4. BEAM CONTAMINATION

The 6–7-MeV photon beam is contaminated by radiation from 4 sources: (i) discrete  $\gamma$ -rays from nuclear reactions induced in the target by the proton beam; (ii) 511-keV  $\gamma$ -rays from positron annihilation after pair-

production events in the target chamber, the surrounding  $\gamma$  filter and the walls of the room; (iii) electrons and positrons created in the target chamber or filter; and (iv) photons scattered from the target chamber and filter. To study these contaminants, a series of experiments was done by changing the filters surrounding the target chamber.

#### 4.1 Discrete $\gamma$ contamination

Figure 5 displays the photon spectrum from the unfiltered target chamber measured with a Ge(Li) counter. The  $\gamma$ -rays near 1.3 MeV and at 110 and 197 keV come from the  $^{19}\text{F}(p,p'\gamma)^{19}\text{F}$  reaction. The other significant peak at 511-keV will be discussed below. Table 1 shows the size of these contaminants for the various filters as a fraction of the 6–7 MeV maximal dose equivalent. These results are deduced from the measured fluences. Two features stand out: (i) the dose equivalent from 511 keV photons is roughly the same in all cases and it is the dominant discrete contaminant; and (ii) the lead filter can virtually eliminate the low-energy ( $p, p'$ ) contaminants. Originally the low-energy contaminants were thought to be much more important and the lead filter was therefore chosen for the "standard" configuration of the source.

#### 4.2 511 keV contamination

With the lead filter in place the 511 keV peak is the largest peak in the spectrum and if it is not an artifact of the response function of the detector, it corresponds to 4.4% of the maximal dose equivalent from 6 to 7 MeV photons. It is very hard to identify the source of these 511 keV  $\gamma$ -rays. They form an almost constant fraction of the high-energy photons as the proton energy is changed and the reaction yields varies by a factor of  $\approx 20$ . As seen in Table 1, various filters have a small effect on the relative intensity of the 511 keV  $\gamma$  peak despite calculated attenuations of 50% or more if the 511 keV photons come through the filter.

The first hypothesis tested was that the 511 keV peak was an artifact of the detector's

Table 1. Discrete  $\gamma$ -ray contaminants as a fraction of the maximal dose equivalent due to 6-7-MeV photons. Values are based on measured fluences converted to maximal dose equivalent using the ANSI conversion factors\* (An77).

Filter	Thickness	Maximal Dose Equivalent as % of 6 to 7 MeV Maximal Dose Equivalent			
		Photon Energy			
		110 keV	197 keV	511 keV	~1.3 MeV
Bare	(~2.6mmFe)	0.6%	2.0%	3.7%	1.2%
Iron	6.4mm	0.2%	1.2%	4.2%	1.1%
Aluminium	10 mm	0.4%	1.6%	3.7%	1.1%
Lead	3.6mm	~0	0.09%	4.4%	1.2%

\*The choice of conversion factors is critical for the low energy region where a factor of 2 difference exists between the ANSI and ICRP conversion factors. The ANSI values produce the larger contamination values.

response, corresponding to pair production events in the detector's container. A study of this possibility by Monte-Carlo calculations has demonstrated that this is not the case and only a small fraction of the 511 keV peak is part of the detector's response (Ro82). Thus the 4.4% dose from the 511 keV peak must be included as part of the calibration field.

About 75% of the 511 keV photons are thought to be from the material near the source target and about 25% from pair production events in the walls of the room and in the air. This was deduced by measuring the change in the ratio of 511 keV counts to counts above 4 MeV in a 2x2 in. NaI crystal when a 1.27 cm lead shield was placed immediately in front of the detector. The ratio changed from 0.21 without the shield to 0.17 with it. Based on the Monte-Carlo calculations for this shielded geometry (described in detail in Ro82) one deduces the breakdown given above for the number of 511 keV photons entering via the front face vs the sides of the detector. Note that while the 1.27 cm lead shield attenuates 511 keV photons in the beam by a factor of 10, pair production by the 7 MeV photons in the beam creates enough 511 keV photons to increase the measured ratio by 0.07. This complicated pattern of attenuation and creation is what makes sorting things out so difficult. A similar result was obtained from measurements of the

ratio of counts with a 4.8 mm lead shield placed around the detector.

Monte-Carlo calculations (described below) have been done to try to isolate the source of the 511 keV photons. However, only a simplified geometry with a point source near a plate is currently available in the Monte-Carlo program. The calculated number of 511 keV photons shows considerable sensitivity to the thickness and the material of the plate whereas experimentally little variation is observed. This lack of variation would suggest that the filters are not the major source of the 511 keV photons.

#### 4.3 Electron contamination

Photons passing through matter set electrons in motion and as the photon energy increases the electrons move more preferentially in the direction of the photon beam. It is thus inevitable that any beam of 6 MeV photons will be contaminated by electrons with energies up to nearly 6 MeV. These can seriously affect an instrument calibration. Furthermore the radiation protection situation will inevitably include similar contaminant electrons which, because of their energy, will contribute to the dose equivalent at depth and not just on the surface.

Several experiments have been performed and will be discussed below to demonstrate

various aspects of this problem. The following factors are worth keeping in mind:

(1) Electrons with energies between 1 and 6 MeV lose 200–250 keV in 100 cm of air and thus the air has little effect on the electrons from the target chamber or filter. On the other hand, Nilsson and Brahme (Ni79) have calculated that the knock-on electrons from the air in a  $20 \times 20$  cm beam of 7 MeV photons will contribute an absorbed dose corresponding to 5% of the peak photon absorbed dose. In the present uncollimated isotropic source geometry this contamination would be higher.

(2) The maximum dose equivalent per particle for electrons with energies between 1 and 6 MeV is 30–100 times larger than for photons of the same energy (ICRP71). Thus even a small electron contamination of the photon beam in terms of fluence can have a large effect on the maximal dose equivalent.

(3) This electron contamination does not have a noticeable effect on the spectra recorded in NaI detectors. Although the NaI detector records virtually every electron hitting it, it also records most photons and thus the effect of the electrons (which have a broad spectrum) is lost in the noise.

**4.3.1 Effects of a build-up cap.** The peak of the absorbed dose vs depth curve for 6–7 MeV photon beams occurs at about  $3.5 \text{ g/cm}^2$  depth because that is roughly the range of 7 MeV electrons. Thus in a pure 6–7 MeV photon beam the response of an ion chamber would be expected to increase as its build-up cap's thickness was increased to  $\sim 3\text{--}4 \text{ g/cm}^2$  and then, on account of scatter, decrease somewhat more slowly than expected from simple photon-attenuation arguments. Figure 7 shows the response of a commonly-used commercial ionization chamber as bakelite is added to its front face. The initial drop off corresponds to the bakelite stopping the contaminant electrons and thereby masking the build-up expected as more photons are detected. This figure implies that the instrument would appear to overrespond as a 6–7 MeV photon detector by about a factor of 2.3 if it has no build-up cap and if the contaminant electrons were

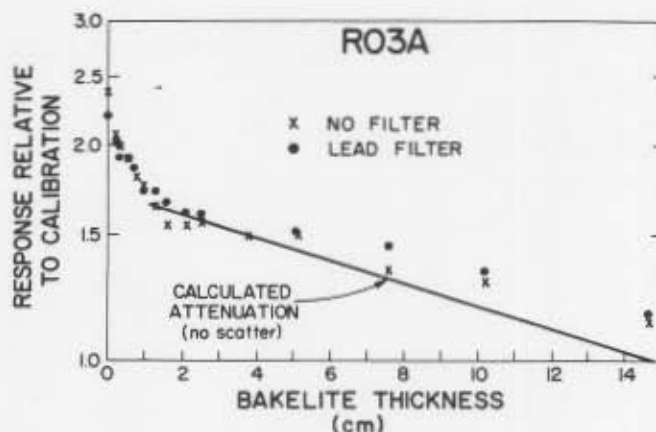


FIG. 7. Response of an Eberline R03A ion chamber as 10 cm squares of bakelite were placed immediately in front of its bare front window. The initial drop off occurs as the contaminant electrons are stopped. The response beyond 4 cm of bakelite is roughly as expected taking into account photon attenuation and scatter. The intermediate response is complicated since contaminant electrons are being removed while the photon dose is building up to its maximum around 2–3 cm depth. The close agreement of the results for the target chamber with or without the lead filter suggests that the filter doesn't change the electron contamination a great deal (as expected) and that the scattered photons do not play a significant role (contrary to expectations). The response is given relative to the 6 and 7 MeV photon maximal dose equivalent as deduced using ICRP21 conversion factors.

ignored. On the other hand, it would still overrespond by a factor of 1.6 with a 2 cm thick build-up cap which would eliminate the contaminant electrons but which would presumably cause an underresponse to lower-energy photons. It must be pointed out that the calibration does not include any estimates of contaminant photons which constitute a 15–20% effect—but the lack of change between the data with and without a lead filter makes a quantitative estimate difficult.

Similar measurements of response vs bakelite thickness were done for an instrument based on a *G-M* tube. No initial drop-off or build-up were observed although the tube was thought to have only about  $100 \text{ mg/cm}^2$  of covering material or less.

**4.3.2 Effects of the source of electrons.** The electron contamination is believed to come primarily from the target

chamber (which has a total of about 2.6 mm of material surrounding the target, mostly steel and copper) and the lead used to filter out low-energy  $\gamma$ -ray contamination. To investigate whether different sources of electrons caused significant effects on instrument response, filters of Pb, Al and Fe were built which were at least thick enough to generate the equilibrium-electron spectrum from that material (2.7–5 g/cm<sup>2</sup>). The filters were cylinders, roughly 10 cm long, which would fit around the target chamber. It was experimentally verified that the filters did not change the source calibration factor since they attenuated both the calibrated beam and photons going to the monitor counter and they did not change the discrete-source spectrum significantly except for the 110 and 197 keV  $\gamma$ -rays.

Measurements were done with an 0.7-l ion chamber constructed entirely of bakelite. A cap was built which surrounded the chamber with 2.5 cm (3.5 g/cm<sup>2</sup>) of bakelite.

It was found that with the cap on, the calibrations, in terms of charge collected per unit 6–7 MeV photons fluence, were independent (within  $\pm 2\%$ ) of which filter was used. This suggests that the 2.5-cm (3.5 g/cm<sup>2</sup>) cap stops all contaminant electrons and the changes in the low-energy  $\gamma$  spectrum are not significant in terms of dose. With the cap off (leaving a 5 mm bakelite wall), the chamber response per unit 6–7 MeV fluence increased in all cases: bare chamber +26%; iron filter +27%; lead filter +33%; aluminium filter +15%. These values are hard to interpret quantitatively since they represent the difference between a decrease on account of lesser build-up (which decreases the calibration factor equally in all cases) and an increase due to electron contamination (which is only partially measured on account of the 5 mm walls). The results demonstrate that the source of the electrons has some effect on the ion-chamber response, but the maximum variation is about 20%. The close agreement between the bare target-chamber results (2.1 g/cm<sup>2</sup> of steel) and the iron-filter results suggests that even the thin steel target-chamber walls create an equilibrium iron spectrum and hence much less

than 3.5 g/cm<sup>2</sup> may be enough to establish an effectively equilibrium-electron spectrum.

*4.3.3 Some electron-photon transport calculations.* The experimental results are difficult to interpret because of the interplay of several effects. In an effort to sort things out, Monte-Carlo calculations were done for a simplified geometry to investigate sensitivity to filter thickness and material. The calculations used the EGS3 Monte-Carlo electron-photon transport system (Fo78; Ne80) and a general purposes user's code called CONVERT. This code determines the number of electrons and photons hitting an arbitrary area at an arbitrary distance from a semi-infinite plate which is irradiated by electrons or photons from a source on the far side of the plate. For the current case the source was 2.5 cm from the plate and collimated to a 6 cm radius on the plate and the electrons and photons crossing a circle 100 cm away subtending a 1 sr cone were counted. The realistic geometry would have the source inside a cylindrical tube, but since electrons from the far side could not penetrate the plate (unlike photons) and since the exiting electron fluence is not sensitive to the plate's depth (past a minimum), it is therefore expected that the calculated electron spectra should be fairly realistic, despite the unrealistic geometry (this does not apply to the calculated photon spectra). The simulations do not track electrons below 190 keV but otherwise, all important physical processes are accounted for in the EGS3 system (Fo78; Ne80; Ro82). A modified electron step size has been found necessary in similar calculations (Ro82b) and has been used here. The current calculations do not include air effects.

Figure 8 presents the calculated electron/positron spectra for 4 material/thickness combinations. Note that the various spectra are not substantially different, the integrated fluences varying from 6.3 to 7.9% of the 7-MeV fluence, respectively, whereas the plate attenuated the primary beam by 6–20%. The lead produces the highest fluence, due almost entirely to the increased importance of pair production in lead.

Using ICRP71 electron-fluence to dose

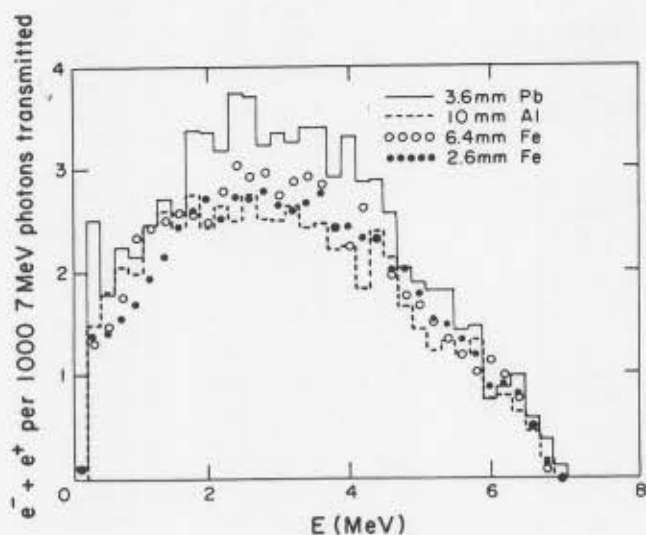


FIG. 8. The calculated spectra of  $e^-$  and  $e^+$  at the calibration position 100 cm from filters of various materials. A simplified geometry was used (see text). A crude estimate of the dose equivalent for the Pb case implies the dose equivalent from the  $e^+$  and  $e^-$  is twice the dose equivalent from the photons.

equivalence conversion factors one finds that the lead electrons and positrons contribute a maximal dose equivalent at 100 cm amounting to twice the maximal dose equivalent from the 7 MeV photons.<sup>†</sup> Values for the other filters would be about 25% lower because of the somewhat smaller electron fluence.

These calculations show that the electrons can be expected to make a substantial contribution to the reading on a survey instrument and a substantial contribution to the dose equivalent delivered by the beam. The exact relationship between the various quantities is virtually impossible to unscramble in a general manner.

<sup>†</sup>For this calculation it was assumed that the maximal dose equivalent for a spectrum is the sum of the maximal dose equivalents for each energy bin. Since the maximum dose equivalent occurs at different depths for different energies, the values are not actually additive and this procedure overestimates the maximum dose equivalent (see Ro79 for a detailed discussion for the case of neutrons).

#### 4.4 Scattered photons

Photons scattered in the filter and material surrounding the target also represent a beam contamination. Although the Monte-Carlo code discussed above also calculates the scattered photon spectrum, the unrealistic geometry of the program means the results are at best a rough guide and likely an underestimate of the actual scattered contribution. The calculations show that there are greater than a factor of three differences in scattered-photon fluences for the various material/thickness combinations reported above. They suggest that the scattered photons would contribute ~6–20% of the maximal dose equivalent from 7 MeV photons and the amount is strongly related to the mass of scattering material considered. This variation was not observed in the present measurements and is under further investigation (Ma82).

#### 4.5 Summary of contaminants

Table 2 presents a summary of the contaminants in the 6–7 MeV calibration field. The calculated 200% electron contamination seems somewhat high based on the data in Fig. 7 but can be seen to be the right order of magnitude if one remembers the photon response for zero thickness of bakelite is expected to be close to zero.

The cap-on measurements for the 0.7-l. ion chamber were constant to within  $\pm 2\%$  for the various filters. With the cap on this chamber does not respond to electrons but would respond to the lower energy contaminant photons. The constant measured value is thus contrary to what is expected based on the variations in values shown in Table 2.

### 5. DISCUSSION

About 10 commercial survey instruments have been calibrated in the 6–7 MeV field and they generally overresponded compared to a <sup>60</sup>Co exposure calibration. The most accurate was a large-volume ion chamber with a 9 mm polyethylene build-up cap. The remaining ion chambers overresponded by between 10 and 70%. Three instruments based on G.M. tubes overresponded by 150%.

Clearly the electron contamination plays an

Table 2. Summary of contaminants in the 6-7 MeV calibration field. Values as a percentage of the maximal dose equivalent delivered by the 6-7 MeV photons. The total maximal dose equivalent would not be the sum of the values for the reasons discussed in the text

Contaminant	Lead Filter		Variation for Other filters
	% Dose Equivalent	How Obtained	
$^{19}\text{F}(p,p')$	1.3%	measured	up to 3.8%
511 keV	4.4%	measured	~ same for all
$e^- + e^+$	203%*	calculation	~ 25% less
scattered gammas	6-20%	calculation	varies from 0.3 to 1.5 times

\*due to electrons above 190 keV only

important role in this over-response. Furthermore, the conversion from a scale reading in mR/h based on a  $^{60}\text{Co}$  exposure-calibration factor to a maximal dose equivalent value for 6 MeV photons has not been included in the above comparisons. For the large ion chambers this is quite difficult. In general we have  $D_{\text{tissue}} = RN_x C_A$ , where  $N_x$  is the  $^{60}\text{Co}$  exposure-calibration factor,  $R$  is the meter reading with the ion chamber in a phantom and  $C_A$  converts from exposure to absorbed dose in tissue. For the NRCC 0.7-l. chamber with its cap on, a very crude estimate gives  $C_A \approx 0.85$  rad/R.

As discussed above, there are also problems with the choice of fluence to dose equivalent conversion factors which vary by 6% at 7 MeV.

The electron contamination poses real, and perhaps insurmountable problems. The choice of the lead filter to eliminate the 110 and 197-keV  $\gamma$ -rays was unfortunate since it increases the electron contamination problem. Even if the filter were eliminated, the measurements and calculations indicate that the bare target chamber is effectively thick as far as electron production is concerned. The target chamber used was a low-mass chamber designed for neutron work and cannot be made too much lighter because direct water cooling of the target is necessary when using 50  $\mu\text{A}$  beams. It thus appears that a significant electron contamination is inevitable and its effect on instrument calibrations will depend dramatically on the instrument's

construction. Furthermore, preliminary calculations indicate that the electron contamination is dependent on the geometric set up as well as the filter materials involved. This makes it virtually impossible to create a calibration set up which represents practical situations.

The present calibration procedure does not take into account electron contamination but methods which do so could be devised, based on calibrated medical ion chambers. The dose at some specified depth in a phantom would be determined—but what should the depth be? These kinds of questions make the problem of how to properly calibrate or specify the field seem virtually intractable and raise fundamental questions about the value of a 6-7 MeV calibration field for instrument calibrations. However, these same problems occur in radiation protection situations and it is hoped that work with the current source can help clarify the situation.

## 6. SUMMARY

A 6-7-MeV  $\gamma$  calibration facility has been developed, based on photons generated by the  $^{19}\text{F}(p, \alpha\gamma)^{16}\text{O}$  reaction. Protons of 2.7 MeV bombard a thick  $\text{CaF}_2$  target and can generate a maximum photon dose equivalent rate of 0.6 mSv/h (600 mrem/h) at 100 cm from the target. The field is uniform over a large area. The calibration is done by measuring the photon fluence and is in principle an absolute calibration. The present source uses a lead filter but this is not neces-

sary and it may be preferable to standardize on another material.

The effects of various filter materials on the beam contaminants have been studied. Experiments demonstrate how hard it is to isolate or quantify individual effects and Monte-Carlo calculations have been used as a guide to what is going on. Unfortunately the effects of contamination are strongly dependent on the particular instrument being calibrated. The electron contamination can produce an absorbed dose as much as twice as large as the absorbed dose from the 6–7-MeV photons.

Work is in progress to compare absolutely the absorbed dose determined from the fluence measurements and that determined with a Baldwin-Farmer ion chamber in a water phantom (Ma82). This work is also attempting to quantitatively estimate the contributions of various contaminants.

*Acknowledgments*—I would like to thank Jack Stinson and George Smith for developing the targets used in this source, Dave Elliott for his excellent help running the accelerator, George Yelle for help using the 0.7-l. ion chamber, Dr. Henryk Mach for assistance collecting data and Drs. Bill Henry and Klaus Geiger for many useful discussions. This work was initiated under a contract from the Central Safety Services Branch of Ontario Hydro in Pickering, Ontario. Finally, I want to acknowledge my old friend  $^{19}\text{F}$  which has been a major element in much of my research career. The idea for this source occurred after years spent in  $\gamma$ -ray spectroscopy research trying to minimize  $^{19}\text{F}$  contamination in nuclear targets in order to avoid 6 MeV  $\gamma$ -rays.

#### REFERENCES

- AN77 American National Standards Institute/American Nuclear Society, 1977, "American National Standard Neutron and Gamma-Ray Flux-To-Dose-Rate Factors", Report ANSI/ANS-6.1.1-1977 (N666).
- Aj77 Ajzenberg-Selove F., 1977, "Energy-Levels of Light Nuclei,  $A = 16, 17$ ", *Nucl. Phys.* **A281**, 1.
- Bi75 Bishop G. B. and Birchall I., 1975, "The  $^{16}\text{N}$  Radiation Shielding Unit at the Universities Research Reactor Centre", *Ann. Nucl. Engng* **2**, 467.
- Cl70 Clairborne H. C. and Trubey D. K., 1970, "Dose Rates in a Slab Phantom from Monoenergetic Gamma-rays", *Nucl. Appl. Tech.* **8**, 450.
- Di81 Dixon W. R. and Storey R. S., 1981, National Research Council of Canada, Ottawa, private communication.
- Fo78 Ford R. L. and Nelson W. R., 1978, "The EGS Code System", Stanford Linear Accelerator Center Report No. 210.
- Go60 Gove H. E. and Litherland A. E., 1960, in: *Nuclear Spectroscopy*, Part A (Edited by Ajzenberg-Selove), p. 260. (New York: Academic Press).
- ICRP71 International Commission on Radiological Protection, 1971, ICRP Publication 21 (Oxford: Pergamon Press).
- ICRU76 International Commission on Radiation Units and Measurements, 1976, ICRU Report 25, "Conceptual Basis for the Determination of Dose Equivalent" (Washington: ICRU).
- Ma82 Mach H. A. and Rogers D. W. O., 1982, National Research Council of Canada, Ottawa, to be published.
- Ne78 Nelson W. R., 1980, various chapters in: *Computer Techniques in Radiation Transport and Dosimetry* (Edited by W. R. Nelson and T. M. Jenkins). (New York: Plenum Press).
- Ne80 Neault P. J., 1980, "The Dosimetry of  $^{16}\text{N}$ " MSc Thesis, University of Lowell.
- Ni79 Nilsson B. O. and Brahme A., 1979, "Absorbed Dose from Secondary Electrons in High Energy Photon Beams", *Phys. Med. Biol.* **24**, 901.
- Ro79 Rogers D. W. O., 1979, "Why Not to Trust a Neutron Remmeter," *Health Phys.* **37**, 735.
- Ro82 Rogers D. W. O., 1982, "More Realistic Monte Carlo Calculations of Photon Detector Response Functions", *Nucl. Inst. Meth.*, **199**, 531.
- Ro82b Rogers D. W. O., 1982, "Use of EGS3 with Low Energy Electrons", National Research Council of Canada, Ottawa, Submitted to *Nucl. Inst. Meth.*
- Ro82c Rogers D. W. O., 1982, "Fluence to Dose Equivalent Conversion Factors for Electrons from 100 keV to 20 GeV and Photons from 20 keV to 20 GeV", National Research Council of Canada, Ottawa, Submitted to *Health Phys.*
- Th71 Thompson I. M. G., Lavender A., Shipton R. G. and Goodwin J., "The Energy Response of Some Commercial Beta/Gamma and Neutron Survey Instruments", in: *Advances in Physical and Biological Radiation Detectors*, p. 505. (Vienna: IAEA).